Atmospheric Environment 228 (2020) 117452

Contents lists available at ScienceDirect

Atmospheric Environment

journal homepage: http://www.elsevier.com/locate/atmosenv

# Quantifying $CH_4$ concentration spikes above baseline and attributing $CH_4$ sources to hydraulic fracturing activities by continuous monitoring at an off-site tower

Sarah J. Russell [a,1], Chante' D. Vines [b], Gil Bohrer [b], Derek R. Johnson [c], Jorge A. Villa [b,2], Robert Heltzel [c], Camilo Rey-Sanchez [b,3], Jaclyn H. Matthes [a,*]

[a] Department of Biological Sciences, Wellesley College, 106 Central St, Wellesley, MA, 02481, United States
[b] Department of Civil, Environmental, and Geodetic Engineering, The Ohio State University, 2070 Neil Ave, Columbus, OH, 43210, United States
[c] Department of Mechanical and Aerospace Engineering, West Virginia University, 1306 Evansdale Dr, PO Box 6106, Morgantown, WV, 26506, United States

## HIGHLIGHTS

- An off-site tower measured CH4 concentrations pre-drilling through fracking.
- A baseline ANN model was developed and extrapolated through fracking phases.
- CH4 concentration spikes were identified by comparing measurements to the model.
- CH4 concentration spikes were largest in vertical drilling and fracking phases.
- Stable isotopes confirmed that CH4 spikes were due to natural gas emissions.

## ARTICLE INFO

*Keywords:*
Methane
Natural gas
Hydraulic fracturing
Artificial neural network

## ABSTRACT

Hydraulic fracturing (hydrofracking) for natural gas has increased rapidly in the area of the Marcellus Shale in the last thirty years and estimates of $CH_4$ emissions from hydrofracking operations are still uncertain. Previous studies on $CH_4$ emissions at hydrofracking operations have used bottom-up approaches collected at discrete timepoints or discrete aerial surveys covering a wide spatial area, constraining the temporal scale of inference regarding these emissions. This project monitored atmospheric $CH_4$ concentrations and stable carbon isotopes at a half-hourly temporal resolution from a 20-m tower downwind of a hydrofracking well pad in West Virginia for eighteen months. We collected four months of baseline observations prior to onsite well development to construct an empirical artificial neural-network model of baseline $CH_4$ concentrations. We compared measured $CH_4$ concentrations against the ANN-modeled $CH_4$ baseline to identify $CH_4$ concentration spikes that coincided with different stages of onsite well development, from the baseline period through fracking. $CH_4$ concentration spikes were significantly more frequent than baseline conditions during the vertical drilling and fracking phases of operations. We found that the median magnitude of $CH_4$ concentration spikes during the vertical drilling phase was 316% larger than that of the baseline phase, and the median magnitude of $CH_4$ concentration spikes was 509% larger in the hydraulic stimulation (fracking) stage compared to the baseline phase. We also partitioned the sources of measured $CH_4$ concentrations to biogenic ruminant and geologic shale gas isotopic signatures by measuring $^{13}CH_4$ gas at high temporal resolution and using a source-partitioning $^{13}CH_4$ model. The measured median value of half-hourly $CH_4$ concentration spikes attributed to a geologic shale gas isotopic origin was 27% larger than the median $CH_4$ concentration spikes attributed to ruminants, and the maximum half-hourly $CH_4$ concentration spike attributed to shale gas was up to 179% higher than maximum $CH_4$ concentration spike for ruminant-dominated half-hours. This study developed a framework for off-site, single tower measurements to

* Corresponding author. 106 Central St., Wellesley, MA, 02481, United States.
*E-mail address:* jmatthes@wellesley.edu (J.H. Matthes).
[1] Present address: Dept. Geography, University of British Columbia, 1984 West Mall, Vancouver, BC V6T 1Z2, Canada.
[2] Present address: School of Geosciences, University of Louisiana at Lafayette, 329 Hamilton Hall, 611 McKinley Street, Lafayette, LA 70504.
[3] Present address: Dept. Environmental Science, Policy, & Management, University of California – Berkeley, 130 Mulford Hall #3114, Berkeley, CA 94720.

https://doi.org/10.1016/j.atmosenv.2020.117452
Received 7 October 2019; Received in revised form 22 March 2020; Accepted 24 March 2020
Available online 30 March 2020
1352-2310/

identify $CH_4$ concentration spikes associated with the phases of unconventional natural gas well development in a complex $CH_4$ emissions airshed.

## 1. Introduction

Methane ($CH_4$) is one of the most important greenhouse gases contributing to climate change. The radiative forcing potential of $CH_4$ is around 26–29 times greater than that of carbon dioxide on a 100-year time scale and methane emissions have a considerable impact on short term climate warming (Intergovernmental Panel on Climate Change, 2014; Prather et al., 2012). Hydraulic fracturing is a method for natural gas extraction that became widespread within the U.S. in the 1990s and has since become common worldwide. The economic value of a single unconventional well pad (*i.e.*, a well pad where hydraulic fracturing occurs) is typically maximized by first drilling vertically, and then horizontally through the shale, allowing natural gas to be extracted from a larger spatial area of the deposit. Natural gas is often considered a cleaner energy source than coal because natural gas drilling is potentially less environmentally destructive and produces less waste (Cathles et al., 2012). Natural gas production also emits fewer greenhouse gases per unit energy produced than does coal, as long as $CH_4$ emissions during fossil fuel extraction and production do not exceed 3.2% of the total natural gas produced (Alvarez et al., 2012).

There have been increasing efforts to identify changes in $CH_4$ and carbon dioxide ($CO_2$) emissions during the construction of unconventional wells and implementation of hydraulic fracturing, and estimates have increased in magnitude during the past decade (Alvarez et al., 2018; Goetz et al., 2017; Omara et al., 2016). Some estimates of methane emissions from unconventional well infrastructure exceed the 3.2% threshold presented by Alvarez et al. (2012), at which the life-cycle carbon footprint of fracked natural gas may exceed that of coal for electricity production. Fugitive $CH_4$ emissions during shale gas extraction can be reduced by implementing green technology solutions during construction and drilling (Cathles et al., 2012; Reay et al., 2018). There is recent evidence to suggest that regulations on $CH_4$ emissions during the completion-venting step of hydraulic fracturing have reduced regional $CH_4$ emissions (Ren et al., 2019). Knowing which stages of unconventional well development emit the most methane could help engineers and policy makers to target and enforce key management practices to reduce fugitive $CH_4$ emissions.

The goal of this study was to develop a monitoring approach that can identify the increased occurrence of fugitive $CH_4$ emissions during different stages of drilling, hydrofracturing and production of at a natural gas well pad. We sought an approach that could be appropriate for a third-party off-site monitoring system, to be used in cases when direct access to the well site is limited or not available. Our approach is based on observing the changes in $CH_4$ concentration spikes before and during unconventional well development. We hypothesized that at a given location, the concentration of $CH_4$ from natural sources can be explained by natural forcing, such as wind speed and direction, and air temperature, which control either the upwind location of potential natural sources or the rate of methane production by natural processes. This hypothesis can be framed as a baseline model of methane concentration as a function of environmental drivers at a given location. A direct prediction from this hypothesis is that, given a long enough observation period for model calibration and in the lack of any new or anthropogenic sources, the distribution of spikes above the baseline model prediction is constant. Any added $CH_4$ sources that were not present during the observation period used to develop the baseline model could be detected through a significant increase in the frequency and intensity of above-model-prediction spikes. In the current project, after measuring and developing a baseline $CH_4$-concentration model, we used model predictions to identify $CH_4$-concentration spikes during the phases of unconventional well development. We verified that these concentration spikes were a result of geologic emissions by measuring continuous isotopic $^{13}CH_4$ values simultaneously with $CH_4$ concentrations.

Previous research has quantified $CH_4$ emissions from fracking sites using a bottom-up approach, usually by measuring single point sources of emissions from hydraulic fracturing infrastructure at a single point in time and using those values to model emissions across the entire process (Allen et al., 2013; Kang et al., 2016; Townsend-Small et al., 2016a,b, 2015). A top-down approach observes total atmospheric methane over a longer time period by co-locating continuous measurements and the potential sources around an unconventional well pad. Previous top-down studies of methane emissions at unconventional well sites have used aerial surveys lasting a few hours during the day, flying through plumes of methane downwind of well pads and creating a map with flight path data showing elevated methane concentrations in a plume originating around the fracking pad (Caulton et al., 2014; Karion et al., 2013; Mitchell et al., 2015; Peischl et al., 2016; Pétron et al., 2014, 2012). Estimates of fugitive emissions derived from top-down measurements were typically higher than those derived from bottom-up measurements, due to the spatiotemporal mismatch in the data collection between these methods (Vaughn et al., 2018).

This study built on the top-down observation approach by observing long-term methane concentrations at a single measurement tower, sacrificing spatial resolution for enhanced temporal resolution and a spatially wide concentration-source footprint. We measured quasi-continuous $CH_4$ concentrations in the boundary layer at a 20 m tower using an in-situ gas analyzer along with high temporal resolution $^{13}CH_4$ isotope concentrations to partition $CH_4$ sources as biogenic or geologic in origin. Observations began at the tower four months prior to onsite well development, which allowed us to optimize a baseline $CH_4$ concentration model using an artificial neural network driven by meteorological and surface flux observations (Baldocchi et al., 2001). Instruments were continuously operated through the phases of hydraulic fracturing, including a baseline pre-drilling period, vertical drilling, horizontal drilling, and fracking (also called hydraulic stimulation).

This study aimed to 1) monitor continuous atmospheric $CH_4$ concentrations downwind of an unconventional well site during a baseline period and through fracking, 2) identify $CH_4$ concentration spikes during the phases of unconventional well development by comparing measured $CH_4$ concentrations with an artificial neural network model trained on the baseline period, and 3) verify that identified $CH_4$ concentration spikes were of geological shale gas origin using direct, continuous isotopic $^{13}CH_4$ measurements with a source partitioning model.

## 2. Methods

### 2.1. Site description

We constructed a 20 m tall eddy covariance tower (39° 40′43 N, 80° 9′52 W) in a grassy meadow (~300 m × 400 m) on a flat hilltop surrounded by deciduous forest in Jakes Run, West Virginia that was approximately 2.5 km northeast of an active well pad site (Fig. 1). The larger area around the tower included deciduous forest, un-grazed grassland, grazed grassland, and a nearby stream. Data collection at the tower began in July 2017, which coincided with the beginning of construction of the well pad site during the baseline period, and monitoring extended through January 2019. Drilling activity at the fracking pad site started late November 2017. Natural gas extraction by hydrofracking first requires vertical drilling into the shale formation followed by horizontal drilling in several lateral directions outward from the central vertical axis. This is followed by fracking (hydraulic stimulation)

where liquid is flushed through the system to extract the natural gas. We sectioned our data into five periods of hydraulic fracturing activity to assess potential differences in $CH_4$ concentrations: baseline (7/1/17–11/17/17), vertical drilling (11/17/17–2/4/18), pause 1 (2/5/18–4/14/19), horizontal drilling (4/15/18–8/8/18), pause 2 (8/9/18–9/12/19), and fracking (hydraulic stimulation; 9/13/18–12/17/18).

A nearby livestock farm and a stream represented the primary potential sources of biogenic methane emissions at this site. Our isotopic partitioning framework accounted for $CH_4$ concentrations originating from livestock, but did not account for other biogenic emissions such as microbes from soils or streams. To check whether nearby soils or the stream were significant sources of $CH_4$ within our tower footprint, we measured surface-atmosphere $CH_4$ chamber flux in June–September 2018 in four ecosystem types: forest floor, grazed pasture, un-grazed field, and stream, with nine replicates per ecosystem type collected in each month. We used a standard chamber construction (as in Villa et al., *Under Review*) and we measured the accumulation of $CH_4$ within the chamber with a mobile gas concentration analyzer (Picarro G4301, Picarro, Santa Clara, CA). These measurements revealed that the surrounding stream and soil were not significant sources of biogenic methane emissions (Supplementary Table S1), so we considered ruminant animals to be the major biogenic source of $CH_4$ within our tower footprint.

### 2.2. Data collection and quality assurance

Data collection at the tower began in July 2017 about four months before drilling activity began at the well pad site in order to measure pre-drilling baseline $CH_4$ concentrations and associated meteorological variables. We deployed an ultrasonic anemometer (CSAT3, Campbell Scientific, Logan, UT) to measure 3-D atmospheric turbulence, an open-path infrared gas analyzer to measure methane concentration (LI-7700, LI-COR Biosciences, Lincoln, NE), and an open-path infrared gas analyzer to measure $CO_2$ and water vapor concentrations (EC-150, Campbell Scientific, Logan, UT). The ultrasonic anemometer and infrared gas analyzers collected data at 10 Hz temporal resolution. The tower also included a net radiometer (NR-Lite, Kipp & Zonnen, Delft, Netherlands) and a temperature and humidity sensor (HMP45g, Vaisala, Vantaa, Finland). Data were logged on a micrologger (CR3000, Campbell Scientific, Logan UT), transmitted to a nearby computer via FM radio, and uploaded to the data cloud via a local Wi-Fi connection. Net radiation, temperature, and humidity data were collected at 1-min resolution were transformed into half-hourly averages.

Surface-atmosphere fluxes of $CO_2$, $H_2O$, and sensible heat were calculated using the eddy-covariance technique following best practices (Lee et al., 2006; Burba and Anderson, 2010) using code written in Matlab R2017b. For full details regarding the flux processing approach, see (Morin et al., 2014b). Briefly, we removed any data value flagged by the internal quality control indicators of the corresponding measurement sensors. For all 10 Hz variables, we identified observation outliers using a threshold of 6 standard deviations within a 2-min moving window and an absolute high and low range of acceptable data. Outliers in the raw 10 Hz data were removed and replaced by NaN. Any half-hour period that was missing more than 50% of the raw observations was treated as missing (replaced with NaN). Major causes of missing data were power loss to the tower, communication failure between the tower and computer, and snow, ice or heavy precipitation that obscured the sensor mirrors or blocked the sensor observation path. Overall, 67% of the $CH_4$ concentration data from the LI-7700 were filtered out or missing.

We also stationed a cavity ring-down spectrometer on the tower to measure $\delta^{13}CH_4$ (Picarro G2201-i Analyzer for Isotopic $CO_2/CH_4$; Precision <0.16‰; Measurement frequency 5 s). In subsequent analysis we used a 30-s rolling average of $CH_4$ concentration and the $\delta^{13}CH_4$ stable isotope ratio collected by this instrument. We filtered out raw measurements of $\delta^{13}CH_4$ that fell outside the −10‰ to −70‰ range, which are theoretically unrealistic and comprised 4.8% of total observations. An additional 36% of the half-hours were missing due to an equipment malfunction, primarily due to power loss at the tower. After filtering, we calculated the half-hourly mean value of $CH_4$ concentration and the $\delta^{13}CH_4$ stable isotope ratio. All the data collected at the tower site is available through Ameriflux, site ID US-JRn https://ameriflux.lbl.gov/sites/siteinfo/US-JRn.

### 2.3. Artificial neural network baseline $CH_4$ concentration model

We used the artificial neural network (ANN) approach to model the baseline $CH_4$ concentrations using data from the baseline period from July 2017 through October 2017. We assumed that observations during

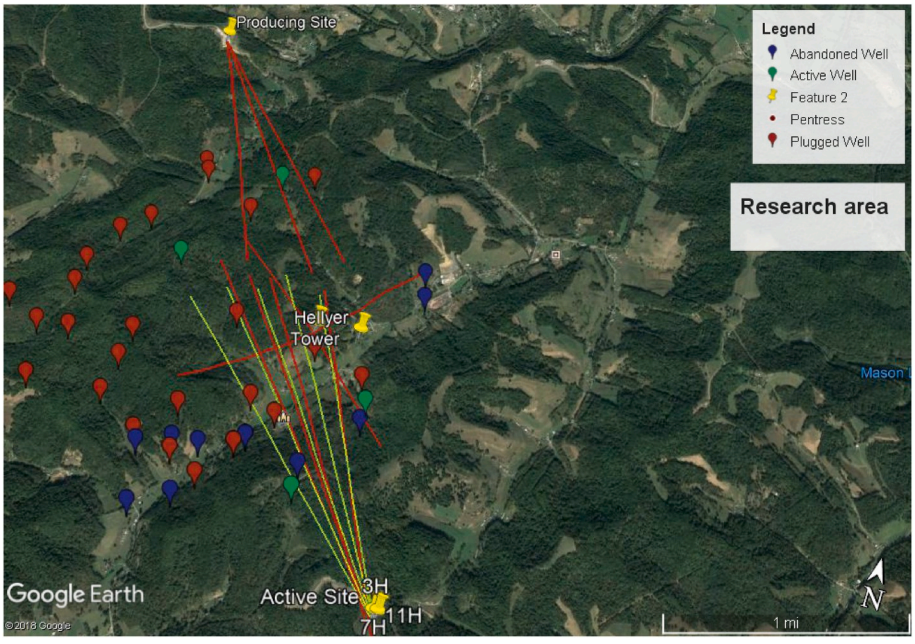


**Fig. 1. West Virginia tower site.** A 20 m tall tower (marked "Tower", near the Hellyer yard) to measure surface-atmosphere exchange was constructed about 2.5 km from the natural gas well pad site (locations 3H, 11H, 7H). An additional producing well is to the north (and typically downwind) of the tower. Previous horizontal drill lines are marked red. Horizontal drill lines that were drilled during the study period are marked yellow. Active, abandoned and plugged wells within 2 km of the tower are marked by location pins. (For interpretation of the references to colour in this figure legend, the reader is referred to the Web version of this article.)

this period represented the baseline concentrations dynamics for this area without the influence of nearby drilling and fracking activities. Large deviations between observed $CH_4$ concentration values and the upper 95% confidence interval of modeled values were identified as concentration spikes. We analyzed the isotopic composition of the spikes to determine their sources, and analyzed the strength and occurrence frequency of spikes during different fracking activity periods. We focused on concentration spikes and not spikes in flux rates because the sporadic and spatially heterogeneous nature of fugitive methane emissions associated with natural gas extraction activities are not compliant with the requirements of eddy-covariance flux measurements. Furthermore, the flux footprint area and distance are much smaller than the concentration footprint (Vesala et al., 2008). Therefore, given the distance between the tower and the drill-pad site, it is most likely that fluxes emitted at the drill-pad where not within the flux footprint area of the eddy-covariance flux measurement but were within the footprint area of the concentration source observations.

The ANN model included an input layer followed by a hyperbolic tangent (tansig) function that produced a hidden layer of 12 nodes. These nodes were then entered into another tansig function that produced a hidden layer of 5 nodes. A final tansig function produced an output layer. While the number of nodes in each layer is arbitrary, this ANN model structure has been successfully used in previous studies for modeling natural methane fluxes (Morin et al., 2014a; Rey-Sanchez et al., 2018), which were likely similar to the baseline $CH_4$ concentrations at our site. The ANN was trained with a randomly selected 50% of baseline period data. We used the ensemble average of the best 100 networks out of 1000 as the final baseline model. A different 25% of the baseline data was used for evaluation to determine the best 10% of the ensemble of 1000 ANN models. The final 25% of baseline data was used for validation of the performance of the resulting ensemble average.

Wind direction, wind speed, water vapor pressure (humidity), air temperature, friction velocity (U*), latent heat flux, sensible heat flux, net ecosystem exchange (NEE) and gross primary production (GPP) were used to train the first layer of the ANN model as environmental drivers of observed $CH_4$ concentration. We chose these variables either because they are directly related to the observation footprint, for example where the concentration that we observed originated from (wind speed, wind direction), or because they are directly related to natural methane production (temperature), or directly related to atmospheric conditions (sensible heat flux, humidity, U*). Finally, we added variables that are strongly correlated with ecosystem function and land cover type (NEE, GPP, latent heat flux) as these may co-vary with natural methane production as well as be indicative of the source footprint. The distribution of ANN-predicted $CH_4$ concentrations from the 100-member ANN ensemble was used to determine the 95% confidence bounds for each predicted half-hourly $CH_4$ concentration. We used gap-filled values of the environmental drivers to provide a continuous time series of input data to the ANN. However, there were no instances where $CH_4$ concentration observations were available but meteorological drivers were missing, and therefore gap-filling the drivers did not affect the training of the baseline methane concentration model since it was only using data when $CH_4$ concentration observations were available. The ANN model was then used to simulate the background $CH_4$ concentration representing baseline conditions for each half-hour during the entire observation period from July 2017 through January 2019. We then compared the ANN-modeled baseline $CH_4$ concentrations to the observed $CH_4$ concentrations. We used this comparison to identify observed $CH_4$ concentration spikes that departed from baseline modeled $CH_4$ concentrations, where we defined a spike as an observed $CH_4$ concentration that fell outside of the upper 95% confidence interval of the ANN-modeled baseline $CH_4$ concentration. Across all of the fracking phases, we tested whether there were significantly more $CH_4$ concentration spikes than expected from the ANN-modeled baseline conditions using a Pearson's chi-squared test.

### 2.4. Miller-Tans isotopic methane source analysis

We used the isotopic $\delta^{13}CH_4$ measurements along with information about background values to partition measured $CH_4$ into biogenic and geologic sources. We used the method developed in Miller and Tans (2003) (modified from Keeling, 1958; reviewed by Pataki et al., 2003) to partition 5-min resolution $\delta^{13}CH_4$ measurements into their dominant $\delta^{13}CH_4$ source value for each half hour interval. This method represents the relationship between an isotopic source and background values as:

$$\delta_{Tot}C_{Tot} - \delta_{Bg}C_{Bg} = \delta_S(C_{Tot} - C_{Bg}) \quad (1)$$

where $C_{Tot}$ and $C_{Bg}$ represent the total and background $CH_4$ concentrations, and $\delta_{Tot}$, $\delta_{Bg}$, and $\delta_S$ represent the $\delta^{13}C$ isotopic ratio of the total, background, and emission source $CH_4$. To use this equation, the background atmospheric $\delta^{13}C$ value ($\delta_{Bg}$) and the background concentration of the gas of interest ($C_{Bg}$) must be provided (Miller and Tans, 2003). We used this method to partition sources of $CH_4$ using the simultaneously measured 5-min $CH_4$ concentrations and $\delta^{13}CH_4$ values from the Picarro G2201-i analyzer.

Several assumptions must be met for Miller-Tans method to be valid: 1) there must be only two possible sources of the gas of interest, which in this study are biogenic ruminant animals and geologic sources related to the production of natural gas, 2) there must be a monotonic increase in the gas of interest during the period used in the analysis, and 3) background atmospheric and source stable isotope ratios are constant throughout the time period (Vardag et al., 2016). We met the last two assumptions by applying the filter criteria outlined in Vardag et al. (2016) to the results of the Miller-Tans plot analysis. To ensure that we analyzed only half-hours where methane had a monotonic increase in concentration, we filtered out half-hours where the range in measured methane concentration was less than 0.1 ppm. We also filtered out half-hours where the standard error of the $\delta^{13}CH_4$ Miller-Tans intercept was more than 2‰, which could have indicated a shift in conditions that changed the emission source isotopic signature during the half-hour window. For all the $CH_4$ concentration and $\delta^{13}CH_4$ data collected, 13% of half-hours were filtered out according to the Miller-Tans filtering criteria outlined in Vardag et al. (2016).

Since we did not directly measure background $\delta^{13}CH_4$ above the boundary layer at our tower, we tested three sources for background atmospheric $\delta^{13}CH_4$ data for our partitioning analysis: 1) well-mixed atmospheric conditions at the tower in this study, and preliminary surface flask $\delta^{13}CH_4$ and concentration data from 2) the Mauna Loa Observatory and 3) Niwot Ridge (Dlugokencky et al., 2018; White et al., 2018). To use background $\delta^{13}CH_4$ data from our tower, we first tested for seasonal and diurnal trends in the $\delta^{13}CH_4$ and $CH_4$ concentration data and then identified well-mixed half-hours by using only the upper quartile half-hours with the fastest measured wind speeds. We averaged these well-mixed half-hours across the entire study period to obtain background methane concentration and $\delta^{13}CH_4$ values. Preliminary flask $\delta^{13}CH_4$ and $CH_4$ concentrations data from the Mauna Loa Observatory and Niwot Ridge were used as alternate background values to measure the sensitivity of our results in response to the choice of background concentration data. There were no seasonal trends in background methane concentrations and $\delta^{13}CH_4$ for well-mixed half-hours at the West Virginia fracking site and from the preliminary surface flask data collected at Mauna Loa and Niwot Ridge (Supplementary Fig. S1A). Due to the low sensitivity of our results to background $\delta^{13}CH_4$ and $CH_4$ values from well-mixed background values at the tower, Niwot Ridge, or Mauna Loa, in our final analysis we used the preliminary $\delta^{13}CH_4$ and $CH_4$ concentration data from Niwot Ridge ($C_{Bg} = 1.91$ ppm, $\delta_{Bg} = -47.43$‰) as the background atmospheric $\delta^{13}CH_4$ ($\delta_{Bg}$) and $CH_4$ concentrations ($C_{Bg}$) (Supplementary Fig. S1B).

To calculate the source $\delta^{13}CH_4$ for each half-hour of data collected at our tower, we used a geometric mean regression that related $C_{Tot}$ - $C_{Bg}$ (the x-axis) to $\delta_{Tot}C_{Tot}$ - $\delta_{Bg}C_{Bg}$ (the y-axis) from Equation (1). The

estimated slope ($\delta_S$) of this regression line represented the source $\delta^{13}CH_4$ and we calculated the standard error of the slope to represent the uncertainty in $\delta_S$ (as described in Miller and Kahn, 1962).

### 2.5. Methane isotopic source partitioning

We used a binomial regression model to categorize the dominant source of methane during each half-hour based on the $\delta^{13}CH_4$ source signature identified by the Miller-Tans analysis. The binomial regression model was constructed with prior distributions of biogenic ruminant and geologic shale gas $\delta^{13}CH_4$ source signatures from data reported in a review of global methane source signatures provided by the NOAA Earth System Research Lab (Sherwood et al., 2017). Since the livestock at our site were fed a mixture of C3 and C4 plants, we combined the distributions of C3-fed and C4-fed ruminants ($\mu_{C3} = -68.39‰$, $SD_{C3} = \pm 3.05‰$; $\mu_{C4} = -54.47$, $SD_{C4} = \pm 3.05$) into a single normal distribution for the prior by averaging their means and adding their standard deviations to get a broad distribution that encompassed both of the original distributions ($\mu = -61.43‰$, $SD = \pm 6.09‰$). For geologic emissions, we used a prior distribution for shale gas produced in the United States ($\mu = -43.90‰$, $SD = \pm 5.90‰$).

Using this binomial regression model and the half-hourly $\delta^{13}CH_4$ source values from the Miller-Tans analysis, we calculated the probability of each half-hour's methane emissions being geologically sourced. The half-hours with a less than 5% geologic source probability were considered to be biogenic livestock dominated and the half-hours with a geologic source probability greater than 95% were considered to be geologic shale gas dominated.

## 3. Results

### 3.1. Patterns in $CH_4$ concentrations and isotopic $\delta^{13}CH_4$ analysis

Measured $CH_4$ concentrations typically ranged from 1.9 to 4 ppm (Fig. 2A) and $\delta^{13}CH_4$ typically ranged from −50 to −45‰ (Fig. 2B). There were no significant seasonal or diurnal trends in measured $CH_4$ and $\delta^{13}CH_4$ concentrations. There were also no significant differences ($p > 0.05$) in the magnitude of the overall mean half-hourly $CH_4$ concentrations nor the overall mean $\delta^{13}CH_4$ isotopic values among each of the four periods of baseline, vertical drilling, horizontal drilling, and hydraulic stimulation (fracking).

Our $\delta^{13}CH_4$ isotopic source partitioning analysis attributed most half-hours to a geologic shale gas source across all measurement periods of this study including the baseline period and different stages of the fracking process, with a high density of source $\delta^{13}CH_4$ centered around −29‰ (Fig. 3). We used the binomial source-partitioning model to classify isotopic $CH_4$ concentrations within half-hours from geologic (shale gas) or biogenic (ruminant) origin. The source partitioning model identified 70% of measured half-hours as being dominated by $CH_4$ from a shale gas origin, 18% of half-hours dominated by $CH_4$ of ruminant origin, and 12% of half-hours with $CH_4$ from an unknown or mixed origin source.

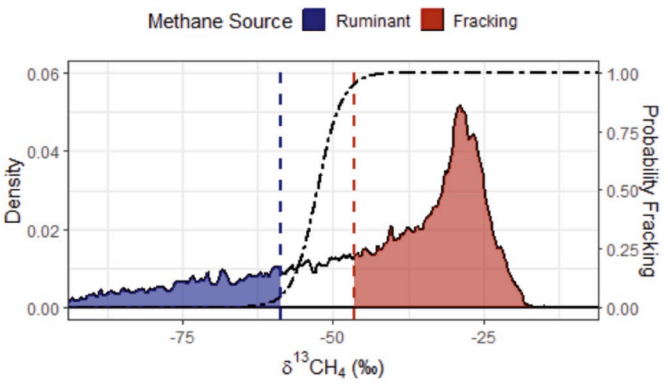


**Fig. 3.** We calculated $\delta^{13}CH_4$ source values for each half-hour with the Miller-Tans method (solid black line). We then used these values in a logistic regression model to partition geologic and biogenic $CH_4$ sources (black dotted line, 1 = shale gas source, 0 = ruminant source). We assigned half-hours to either a geologic source (red shaded area) or a ruminant source (blue shaded area) where the probability of that source was greater than 95%. (For interpretation of the references to colour in this figure legend, the reader is referred to the Web version of this article.)

### 3.2. Comparison between ANN modeled $CH_4$ concentrations and measurements

The ANN model for $CH_4$ concentrations was trained on baseline pre-drilling data and was used to project baseline conditions through the end of the study period (Fig. 4). The model fit the data relatively well with $r^2 = 0.55$ for the validation dataset (25% of half-hourly concentration observations during the baseline period that were not included in model parameterization). We compared measured half-hourly $CH_4$ concentrations to the half-hourly ANN baseline model, and we classified $CH_4$ concentration spikes as measured values that exceeded the upper 95% confidence bound of the ANN baseline model output. This criterion classified 25% of the half-hours during the study period as $CH_4$ concentration spikes within the usable data.

The lowest proportion of measured half-hours classified as $CH_4$ concentration spikes occurred in the baseline period (24% of measured half-hours) and the highest proportion of $CH_4$ concentration spikes occurred during the fracking period (35% of measured half-hours) (Fig. 5A). 29% of measured half-hours were classified as $CH_4$ concentration spikes in the vertical drilling phase and 26% of measured half-hours experienced $CH_4$ concentration spikes in the horizontal drilling phase. We calculated the magnitude of the $CH_4$ concentration spikes as

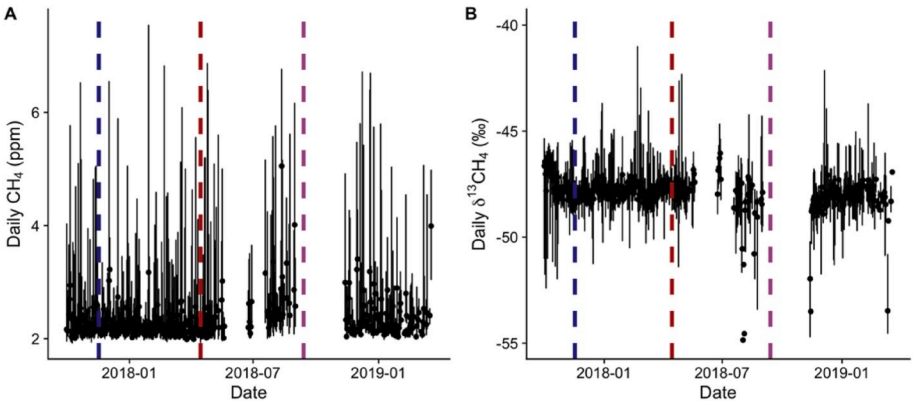


**Fig. 2.** Measured $CH_4$ concentration (A) and isotope $\delta^{13}CH_4$ values (B) during the study period, where points represent the daily median value and lines represent the daily range. The dashed blue line represents the start of vertical drilling, the dashed red line indicates the start of horizontal drilling, and the dashed purple line marks the start of hydraulic stimulation (fracking). There were no significant differences in half-hourly mean $CH_4$ concentration nor $\delta^{13}CH_4$ among the baseline, vertical drilling, horizontal drilling, and fracking periods. (For interpretation of the references to colour in this figure legend, the reader is referred to the Web version of this article.)

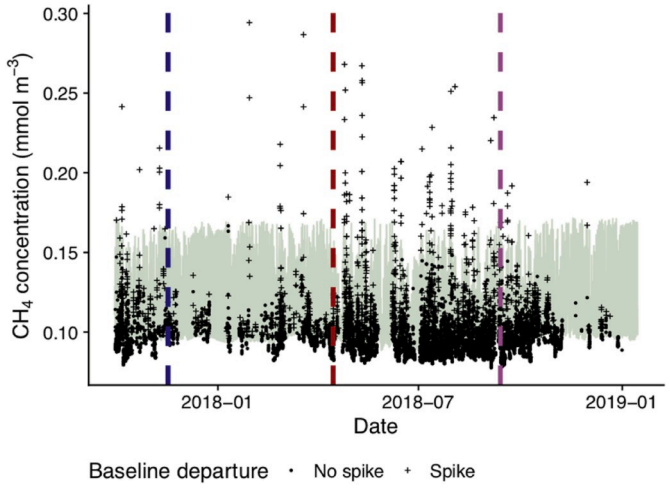


**Fig. 4.** We used an artificial neural network (ANN) model (light green lines) trained on the pre-drilling baseline period to identify measured half-hourly mean $CH_4$ concentrations (black dots and crosses) that were larger than the upper 95% confidence interval of the ANN model. Crosses represent observed values that are larger than the 95% confidence interval of the ANN model results that were categorized as spikes. The dashed blue line represents the start of vertical drilling, the dashed red line indicates the start of horizontal drilling, and the dashed purple line marks the start of hydraulic stimulation (fracking). (For interpretation of the references to colour in this figure legend, the reader is referred to the Web version of this article.)

the difference between the measured $CH_4$ concentration and the ANN modeled $CH_4$ concentration for each half-hour that was flagged as a spike (where the observed concentration was larger than the upper 95% confidence bound of the ANN prediction). We found that the magnitude of the concentration spikes significantly increased during the vertical drilling and fracking periods (Fig. 5B) compared to other periods (Pearson's chi-squared test, $\chi^2 = 31.7$, $df = 5$, significance $p < 0.001$). Compared to the baseline period, the median half-hourly departure from the baseline ANN model was 316% larger during vertical drilling, 9.4% larger during horizontal drilling, and 506% larger during fracking. Both skewness and kurtosis of the $CH_4$ concentration departure values increased during the vertical drilling and fracking periods compared to the baseline period, which indicated a general shift towards larger $CH_4$ concentration spikes during these time periods.

### 3.3. Isotopic source attribution and $CH_4$ concentration spikes

We combined our results from the $CH_4$ concentration spike identification that compared the difference between measured and ANN-modeled half-hourly $CH_4$ concentrations with the isotopic source partitioning analysis to determine the extent to which $CH_4$ concentration spikes were associated with ruminant and shale gas sources (Fig. 6). We found that the majority of $CH_4$ concentration spikes (70% of all classified spikes) were from a shale gas source, with 18% of classified $CH_4$ concentration spikes from a ruminant source and the remaining 12% from a mixed or unknown source. In particular, nearly all of the $CH_4$ concentration spikes with the largest magnitude (*i.e.*, a large measured departure from baseline) were classified as a shale gas origin (Fig. 6). The median size of $CH_4$ concentration spikes in half-hours attributed to shale gas were 27% larger than the magnitude of $CH_4$ concentration spikes from half-hours attributed to ruminants. The maximum $CH_4$ concentration spike in a half-hour dominated by a shale gas source was 179% larger than the maximum $CH_4$ concentration spike in a half-hour with a ruminant $CH_4$ source.

## 4. Discussion

Accurately estimating changes in $CH_4$ dynamics during unconventional well development (*i.e.*, hydrofracking for natural gas) has been challenging due to the complexity of measured $CH_4$ emissions sources, their temporally intermittent nature, the typically small source locations, and due to the temporal and spatial scales required for monitoring. Other challenges stem from the fact that in most areas where hydrofracking occurs, some gas or oil extraction activity is already active in other sites nearby. Well operators are not required to monitor methane emissions, and in almost all cases, they will not allow such monitoring

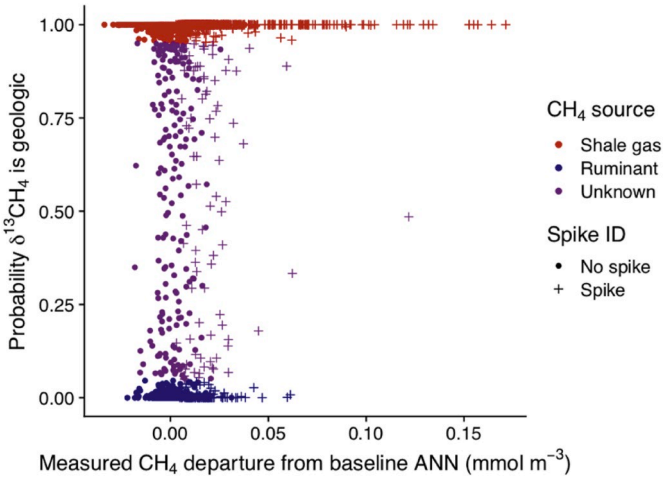


**Fig. 6.** The majority (70%) of the $CH_4$ concentration spikes that were identified by comparison with the artificial neural network baseline model were classified as being of geologic (shale gas) origin from the isotope source-partitioning analysis. Large magnitude $CH_4$ concentration spikes, in particular, were attributed to a shale gas isotopic source.

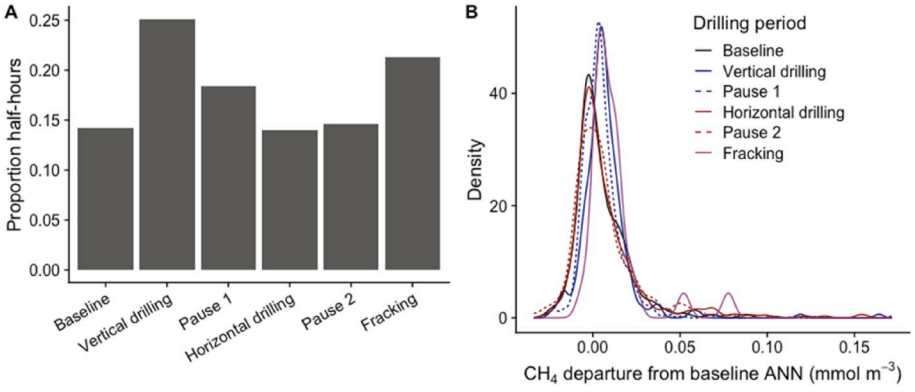


**Fig. 5.** A) The proportion of measured half-hours that were classified as $CH_4$ concentration spikes were significantly higher than baseline estimates during and immediately following the vertical drilling phase and during the fracking phase of operations. B) The magnitude of the $CH_4$ concentration spikes significantly increased during the vertical drilling and fracking periods compared to the pre-drilling baseline period. The horizontal drilling period was not statistically different from the baseline period.

on their property for reasons of safety and liability. Spatially heterogeneous point sources of $CH_4$, for example well pads, prohibit the use of eddy covariance theory for directly measuring $CH_4$ flux in a tower footprint. As a result, most efforts to date used mobile measurements, downwind or near the fence-line of location where natural-gas extraction occurs, either from airborne platform covering large areas (Caulton et al., 2014; Karion et al., 2013; Mitchell et al., 2015; Peischl et al., 2016; Pétron et al., 2014, 2012), or from vehicles (*e.g.,* Eapi et al., 2014; Williams et al., 2018). A recent mobile ship-based study quantified the spatially heterogeneous $CH_4$ emissions from offshore oil and gas platforms with isotopic $^{13}CH_4$ measurements (Yacovitch et al., 2020). While mobile observations can cover large areas, they are intrinsically intermittent and cover very small observational time periods. Combined with the intermittent nature of fugitive emissions, mobile observations can typically detect large emission sources, but cannot necessarily characterize generally small difference in emission incidence between different activity periods. They may also miss large but short-termed events. Other land-based approaches used a large sampling grid (Swarthout et al., 2020) or large meta-analysis of multiple ground-based and airborne observations (Miller et al., 2013) to locate potential emission sources. However, these large observation arrays require extensive effort and are therefore very limited.

This study developed a framework for continuous ground-based monitoring from a single observation tower of changes in $CH_4$ concentration dynamics that are indicative of increased rate and incidence of fugitive emissions using a tower 2.5 km downwind of an active well pad. Our approach is centered on comparison between the concentration dynamics during a baseline period, before the activity in the target upwind pad started (prior to well development) and through the phases of fracking operations. A primary goal in our project was to evaluate the ability of off-site measurements to identify changes in $CH_4$ dynamics that were associated with changes in fracking activities at a locations where on-site, direct and continuous access to well pads was impossible. Previous studies have used single-tower, downwind observations of volatile compounds (VOC) related to natural gas extraction (Helmig et al., 2014) or the isotopic composition of methane (Tyler et al., 2007; Röckmann et al., 2016). In these studies, they attributed the elevated presence of VOC or methane isotopes to the contribution from fracking activity but did not analyze the temporal patterns of the emissions. Our approach allows characterization of the temporal patterns of emission spikes and identification of the period where emissions were elevated relative to a baseline, but cannot directly evaluate the source emission rates. Atmospheric dispersion inversion models, based on plume assumptions, or computational fluid dynamics (*e.g.* large eddy simulations) could hypothetically infer the source emissions rate from our tower observations. However, such model-based inference comes at the cost of added uncertainty due to model error and uncertainty in forcing, initial conditions and domain description parameters at high enough resolution (Caulton et al., 2018).

By developing a baseline model with our pre-drilling $CH_4$ concentration data, we identified $CH_4$ concentration spikes that occurred during the different phases of well-development operations. We found significantly larger $CH_4$ concentration spikes during the vertical drilling and fracking phases of operations, but not during the horizontal drilling phase (Fig. 6). Interestingly, we found that there were larger $CH_4$ concentration spikes in the time period following vertical drilling while no major activities were occurring ("Pause 1" in Fig. 6), which indicated a potential lag effect of vertical drilling that elevated concentration spikes even after drilling had stopped. We hypothesize that these spikes are related to fugitive emissions from the well, during the vertical drilling and shortly after. Likewise, we did not find elevated $CH_4$ concentrations during the pause in operations following horizontal drilling, when $CH_4$ concentration spikes were similar to baseline conditions. Together, this suggested that $CH_4$ concentration dynamics are potentially lagged at the timescale of weeks following the fracking phases that release $CH_4$. With this $CH_4$ concentration spike analysis, we paired an isotopic source partitioning analysis to test whether half-hourly $CH_4$ concentration spikes were dominated by either ruminant animal or shale gas concentration sources.

In this study we did not find absolute differences in the overall half-hourly mean $CH_4$ concentrations nor isotopic $\delta^{13}CH_4$ values throughout the baseline, vertical drilling, horizontal drilling, and fracking periods of our study (Fig. 2). We found significantly more frequent $CH_4$ concentration spikes compared to the baseline period (14% of measured half-hours) in the vertical drilling phase (25% of measured half-hours), the pause in operations following vertical drilling (18% of measured half-hours), and the fracking phase (21% of measured half-hours) (Fig. 5A). Although $CH_4$ concentration spikes were only 7–11% more frequent during the vertical drilling and fracking periods compared to the baseline period, the magnitude of the $CH_4$ concentration spikes during the vertical drilling phase (316% larger median spike $CH_4$ concentration) and fracking phase (506% larger median spike $CH_4$ concentration) were significantly larger than the size of the $CH_4$ spikes that occurred during the baseline phase. During the vertical drilling period, operators often encounter pockets of $CH_4$ within the shallow shale formation that must be released as they drill through the shallow conventional shale depths to the deeper unconventional shale depths. These shallow pockets of gas must be vented and/or flared in order to continue drilling operations, and this could explain the larger magnitude of $CH_4$ concentration spikes during this period of activity. During the fracking (hydraulic stimulation) phase, fugitive $CH_4$ might escape from operations as the rock is fractured to extract $CH_4$ from the natural gas deposits. Repeated mobile measurements of $CH_4$ emissions at oil and gas pads in Texas, Colorado, and Wyoming found similar temporal dynamics to those in our study, where $CH_4$ emissions were low most of the time but had large episodic releases associated with venting (Brantley et al., 2014). Other studies in the Marcellus Shale region also found higher rates of $CH_4$ emission during the drilling phases of operations, likely due to the venting release of methane pockets (Goetz et al., 2015). An airborne regional study of $CH_4$ emission rates from fracking well pads in the Marcellus Shale also found the highest rates of $CH_4$ emissions during the drilling phase of operations, which accounted for 4–30% of total regional $CH_4$ emissions (Caulton et al., 2014). In our study, we found that the distribution of the magnitude of $CH_4$ concentration spikes during the vertical drilling and fracking phases increased in skewness and kurtosis, which demonstrated a significant shift of the median $CH_4$ concentration spike to the right with a longer tail to the distribution for particularly large spikes. These $CH_4$ concentration spike characteristics (the changes in median, skewness, and kurtosis) could serve as helpful data-driven statistical markers of changes in $CH_4$ sources identified by continuous $CH_4$ concentration monitoring networks with off-site towers such as those in this study.

Our isotopic source partitioning analysis confirmed that the large majority (70%) of measured $CH_4$ concentration spikes were of shale gas isotopic origin (Fig. 6). Another study in the Colorado Front Range used carbon and hydrogen isotopes to separate biologic and geologic sources of $CH_4$, but found that $^{13}CH_4$ alone was unable to successfully identify geologic emissions likely due to the combined signatures of both oil and gas production in background samples (Townsend-Small et al., 2016a, b). Other work has shown that the $^{13}CH4$ isotopic value of natural gas shows a thermogenic origin in comparison to a biogenic microbial origin for oil, complicating the partitioning for their combined isotopic profile (Lopez et al., 2017). In contrast, it is likely that our study was able to separate geologic and biogenic sources with $^{13}CH_4$ due to the relative isotopic uniformity of a single shale gas source and due to the long time series of quasi-continuous isotopic measurements. Our results highlighted the potential for a shale gas source to emit much larger amounts of $CH_4$ to the atmosphere within the airshed of the tower compared to the smaller shift in $CH_4$ concentrations that increased with biogenic ruminant activity. All of the largest measured $CH_4$ concentration spikes in our data were of shale gas origin (Fig. 6), where the overall median size of a $CH_4$ spike from a shale gas origin was 27% larger than that of a

ruminant origin. That said, there was a non-negligible source of ruminant $CH_4$ emissions in the study area, which this analysis classified through the paired $CH_4$ concentration spike analysis and isotopic source partitioning model (Fig. 6). Our reliance on literature values for the isotopic source partitioning into ruminant or shale gas origin for the $CH_4$ concentration provided a conservative estimate, since the literature values capture the full measured variation in emissions. This highlights the potential for using this approach in areas where directly measuring point source emissions is impossible, even in tower airsheds with a complex set of point-source $CH_4$ emitters, such as the ruminants and well pads in this study.

## 5. Conclusions

This study developed a framework for monitoring the increased occurrence of fugitive emissions from natural gas production activities by observing changes in $CH_4$ concentration spikes during different phases of fracking operations at an off-site tower 2.5 km away from the well pad under development and compared these $CH_4$ concentration spikes to a baseline-concentration model. The baseline concentration model was driven by meteorological conditions and surface heat, water vapor, and $CO_2$, and was fitted during a season-long period before natural gas extraction started in the target location. Isotopic $\delta^{13}CH_4$ measurements and a source-partitioning model driven with literature values of $\delta^{13}CH_4$ sources confirmed that the majority of $CH_4$ concentration spikes were associated with shale gas sources rather than ruminant sources. We found that the majority of $CH_4$ concentration spikes were of shale gas origin, and all of the very large magnitude spikes had a shale-gas $\delta^{13}CH_4$ fingerprint. The airshed of this monitoring tower represents a complex set of point-source $CH_4$ emission sources, both from cattle and the well pad. This approach of monitoring changes in $CH_4$ concentration spikes relative to a baseline model could be useful as a passive method for continuous off-site monitoring, where direct access to natural gas well pads is restricted or impossible. While quantifying a complete budget of $CH_4$ flux will require additional measurements and inversion models, which come with additional uncertainty, this framework could be useful in identifying statistical characteristics of changes associated with fugitive $CH_4$ emissions during different periods of fracking operations.

## Data availability

All the data collected at the tower site is available through Ameriflux, site ID US-JRn https://ameriflux.lbl.gov/sites/siteinfo/US-JRn.

## Declaration of competing interest

The authors declare that they have no known competing financial interests or personal relationships that could have appeared to influence the work reported in this paper.

## CRediT authorship contribution statement

**Sarah J. Russell:** Methodology, Software, Visualization, Writing - original draft. **Chante' D. Vines:** Methodology, Software, Visualization, Writing - original draft. **Gil Bohrer:** Conceptualization, Methodology, Project administration, Software, Writing - review & editing. **Derek R. Johnson:** Investigation, Data curation, Project administration, Writing - review & editing. **Jorge A. Villa:** Investigation, Software. **Robert Heltzel:** Investigation, Data curation. **Camilo Rey-Sanchez:** Investigation, Software. **Jaclyn H. Matthes:** Conceptualization, Methodology, Software, Supervision, Writing - review & editing.

## Acknowledgements

The study was funded by NSF awards CBET 1508994 and 1509297 and by the Ohio Water Resources Center award G16AP00076. We thank two anonymous reviewers, whose feedback substantially improved this manuscript.

## Appendix A. Supplementary data

Supplementary data to this article can be found online at https://doi.org/10.1016/j.atmosenv.2020.117452.

## References

Allen, D.T., Torres, V.M., Thomas, J., Sullivan, D.W., Harrison, M., Hendler, A., Herndon, S.C., Kolb, C.E., Fraser, M.P., Hill, A.D., Lamb, B.K., Miskimins, J., Sawyer, R.F., Seinfeld, J.H., 2013. Measurements of methane emissions at natural gas production sites in the United States. Proc. Natl. Acad. Sci. U. S. A 110, 17768–17773.

Alvarez, R.A., Pacala, S.W., Winebrake, J.J., Chameides, W.L., Hamburg, S.P., 2012. Greater focus needed on methane leakage from natural gas infrastructure. Proc. Natl. Acad. Sci. U. S. A 109, 6435–6440.

Alvarez, R.A., Zavala-Araiza, D., Lyon, D.R., Allen, D.T., Barkley, Z.R., Brandt, A.R., Davis, K.J., Herndon, S.C., Jacob, D.J., Karion, A., Kort, E.A., Lamb, B.K., Lauvaux, T., Maasakkers, J.D., Marchese, A.J., Omara, M., Pacala, S.W., Peischl, J., Robinson, A.L., Shepson, P.B., Sweeney, C., Townsend-Small, A., Wofsy, S.C., Hamburg, S.P., 2018. Assessment of methane emissions from the U.S. oil and gas supply chain. Science. https://doi.org/10.1126/science.aar7204.

Baldocchi, D., Falge, E., Gu, L., Olson, R., Hollinger, D., Running, S., Anthoni, P., Bernhofer, C., Davis, K., Evans, R., Fuentes, J., Goldstein, A., Katul, G., Law, B., Lee, X., Malhi, Y., Meyers, T., Munger, W., Oechel, W., Paw U, K.T., Pilegaard, K., Schmid, H.P., Valentini, R., Verma, S., Vesala, T., Wilson, K., Wofsy, S., 2001. FLUXNET: a new tool to study the temporal and spatial variability of ecosystem-scale carbon dioxide, water vapor, and energy flux densities. Bull. Am. Meteorol. Soc. 82, 2415–2434.

Brantley, H.L., Thoma, E.D., Squier, W.C., Guven, B.B., Lyon, D., 2014. Assessment of methane emissions from oil and gas production pads using mobile measurements. Environ. Sci. Technol. 48 (24), 14508–14515. https://doi.org/10.1021/es503070q.

Burba, G., Anderson, D., 2010. A Brief Practical Guide to Eddy Covariance Flux Measurements: Principles and Workflow Examples for Scientific and Industrial Applications. LI-COR Biosciences.

Cathles, L.M., Brown, L., Taam, M., Hunter, A., 2012. A commentary on "The greenhouse-gas footprint of natural gas in shale formations" by R.W. Howarth, R. Santoro, and Anthony Ingraffea. Climatic Change 113, 525–535.

Caulton, D.R., Shepson, P.B., Santoro, R.L., Sparks, J.P., Howarth, R.W., Ingraffea, A.R., Cambaliza, M.O.L., Sweeney, C., Karion, A., Davis, K.J., Stirm, B.H., Montzka, S.A., Miller, B.R., 2014. Toward a better understanding and quantification of methane emissions from shale gas development. Proc. Natl. Acad. Sci. U. S. A 111, 6237–6242.

Caulton, D.R., Li, Q., Bou-Zeid, E., Fitts, J.P., Golston, L.M., Pan, D., Lu, J., Lane, H.M., Buchholz, B., Guo, X., McSpiritt, J., Wendt, L., Zondlo, M.A., 2018. Quantifying uncertainties from mobile-laboratory-derived emissions of well pads using inverse Gaussian methods. Atmos. Chem. Phys. 18, 15145–15168. https://doi.org/10.5194/acp-18-15145-2018.

Dlugokencky, E.J., Lang, P.M., Crotwell, A.M., Mund, J.W., Crotwell, M.J., Thoning, K.W., 2018. Atmospheric Methane Dry Air Mole Fractions from the NOAA ESRL Carbon Cycle Cooperative Air Sampling Network 1983-2017.

Eapi, G.R., Sabnis, M.S., Sattler, M.L., 2014. Mobile measurement of methane and hydrogen sulfide at natural gas production site fence lines in the Texas Barnett Shale. J. Air Waste Manag. Assoc. 8, 927–944. https://doi.org/10.1080/10962247.2014.907098.

Goetz, J.D., Floerchinger, D., Fortner, E.C., Wormhoudt, J., Massoli, P., Knighton, W.B., Herndon, S.C., Kolb, C.E., Knipping, E., Shaw, S.L., DeCarlo, P.F., 2015. Atmospheric emission characterization of Marcellus shale natural gas development sites. Environ. Sci. Technol. 49 (11), 7012–7020. https://doi.org/10.1021/acs.est.5b00452.

Goetz, J.D., Douglas Goetz, J., Avery, A., Werden, B., Floerchinger, C., Fortner, E.C., Wormhoudt, J., Massoli, P., Herndon, S.C., Kolb, C.E., Berk Knighton, W., Peischl, J., Warneke, C., De Gouw, J.A., Shaw, S.L., DeCarlo, P.F., 2017. Analysis of local-scale background concentrations of methane and other gas-phase species in the Marcellus Shale. Elem Sci Anth 5, 1. https://doi.org/10.1525/elementa.182.

Helmig, D., Thompson, C.R., Evans, J., Boylan, P., Hueber, J., Park, J.-H., 2014. Highly elevated atmospheric levels of volatile organic compounds in the Uintah Basin, Utah. Environ. Sci. Technol. 48 (9), 4707–4715. https://doi.org/10.1021/es405046r.

Intergovernmental Panel on Climate Change, 2014. Climate Change 2013 – the Physical Science Basis: Working Group I Contribution to the Fifth Assessment Report of the Intergovernmental Panel on Climate Change. Cambridge University Press.

Kang, M., Christian, S., Celia, M.A., Mauzerall, D.L., Bill, M., Miller, A.R., Chen, Y., Conrad, M.E., Darrah, T.H., Jackson, R.B., 2016. Identification and characterization of high methane-emitting abandoned oil and gas wells. In: Proceedings of the National Academy of Sciences. https://doi.org/10.1073/pnas.1605913113.

Karion, A., Sweeney, C., Pétron, G., Frost, G., Michael Hardesty, R., Kofler, J., Miller, B.R., Newberger, T., Wolter, S., Banta, R., 2013. Methane emissions estimate from airborne measurements over a western United States natural gas field. Others Geophys. Res. Lett. 40, 4393–4397.

Keeling, C.D., 1958. The concentration and isotopic abundances of atmospheric carbon dioxide in rural areas. Geochem. Cosmochim. Acta 13, 322–334.

Lee, X., Massman, W., Law, B., 2006. Handbook of Micrometeorology: A Guide for Surface Flux Measurement and Analysis. Springer Science & Business Media.

Lopez, M., Sherwood, O.A., Dlugokencky, E.J., Kessler, R., Giroux, L., Worthy, D.E.J., 2017. Isotopic signatures of anthropogenic CH4 sources in Alberta, Canada. Atmos. Environ. 164, 280–288. https://doi.org/10.1016/j.atmosenv.2017.06.021.

Miller, R.L., Kahn, J.S., 1962. Statistical Analysis in the Geological Sciences. Wiley, New York xiv + 483 pp.

Miller, J.B., Tans, P.P., 2003. Calculating isotopic fractionation from atmospheric measurements at various scales. Tellus B 55, 207–214.

Miller, S.M., Wofsy, S.C., Michalak, A.M., Kort, E.A., Andrews, A.E., Biraud, S.C., Dlugokencky, E.J., Eluszkiewicz, J., Fischer, M.L., Janssens-Maenhout, G., Miller, B. R., Miller, J.B., Montzka, S.A., Nehrkorn, T., Sweeney, C., 2013. Anthropogenic emissions of methane in the United States. Proc. Natl. Acad. Sci. U. S. A. 110 (50), 20018–20022. https://doi.org/10.1073/pnas.1314392110.

Mitchell, A.L., Tkacik, D.S., Roscioli, J.R., Herndon, S.C., Yacovitch, T.I., Martinez, D.M., Vaughn, T.L., Williams, L.L., Sullivan, M.R., Floerchinger, C., Omara, M., Subramanian, R., Zimmerle, D., Marchese, A.J., Robinson, A.L., 2015. Measurements of methane emissions from natural gas gathering facilities and processing plants: measurement results. Environ. Sci. Technol. https://doi.org/10.1021/es5052809.

Morin, T.H., Bohrer, G., Frasson, R.P.d.M., Naor-Azreli, L., Mesi, S., Stefanik, K.C., Schäfer, K.V.R., 2014a. Environmental drivers of methane fluxes from an urban temperate wetland park. J. Geophys. Res. Biogeosci. 119, 2188–2208.

Morin, T.H., Bohrer, G., Naor-Azrieli, L., Mesi, S., Kenny, W.T., Mitsch, W.J., Schäfer, K. V.R., 2014b. The seasonal and diurnal dynamics of methane flux at a created urban wetland. Ecol. Eng. 72, 74–83.

Omara, M., Sullivan, M.R., Li, X., Subramanian, R., Robinson, A.L., Presto, A.A., 2016. Methane emissions from conventional and unconventional natural gas production sites in the Marcellus shale basin. Environ. Sci. Technol. 50 (4), 2099–2107. https://doi.org/10.1021/acs.est.5b05503.

Pataki, D.E., Ehleringer, J.R., Flanagan, L.B., 2003. The Application and Interpretation of Keeling Plots in Terrestrial Carbon Cycle Research (Global).

Peischl, J., Karion, A., Sweeney, C., Kort, E.A., Smith, M.L., Brandt, A.R., Yeskoo, T., Aikin, K.C., Conley, S.A., Gvakharia, A., 2016. Quantifying atmospheric methane emissions from oil and natural gas production in the Bakken shale region of North Dakota. Others J. Geophys. Res. Atmos. 121, 6101–6111.

Pétron, G., Frost, G., Miller, B.R., Hirsch, A.I., Montzka, S.A., Karion, A., Trainer, M., Sweeney, C., Andrews, A.E., Miller, L., 2012. Hydrocarbon emissions characterization in the Colorado Front Range: a pilot study. Others J. Geophys. Res. Atmos. 117.

Pétron, G., Karion, A., Sweeney, C., Miller, B.R., Montzka, S.A., Frost, G.J., Trainer, M., Tans, P., Andrews, A., Kofler, J., 2014. A new look at methane and nonmethane hydrocarbon emissions from oil and natural gas operations in the Colorado Denver-Julesburg Basin. Others J. Geophys. Res. Atmos. 119, 6836–6852.

Prather, M.J., Holmes, C.D., Hsu, J., 2012. Reactive greenhouse gas scenarios: systematic exploration of uncertainties and the role of atmospheric chemistry. Geophys. Res. Lett. 39, L09803.

Reay, D.S., Smith, P., Christensen, T.R., James, R.H., Clark, H., 2018. Methane and global environmental change. Annual review of environment and Resources. https://doi.org/10.1146/annurev-environ-102017-030154.

Ren, X., Hall, D.L., Vinciguerra, T., Benish, S.E., Stratton, P.R., Ahn, D., et al., 2019. Methane emissions from the Marcellus Shale in Southwestern Pennsylvania and northern West Virginia based on airborne measurements. J. Geophys. Res.: Atmosphere 124, 1862–1878. https://doi.org/10.1029/2018JD029690.

Rey-Sanchez, A.C., Morin, T.H., Stefanik, K.C., Wrighton, K., Bohrer, G., 2018. Determining total emissions and environmental drivers of methane flux in a Lake Erie estuarine marsh. Ecol. Eng. 114, 7–15.

Röckmann, T., Eyer, S., van der Veen, C., Popa, M.E., Tuzson, B., Monteil, G., Houweling, S., Harris, E., Brunner, D., Fischer, H., Zazzeri, G., Lowry, D., Nisbet, E. G., Brand, W.A., Necki, J.M., Emmenegger, L., Mohn, J., 2016. In situ observations of the isotopic composition of methane at the Cabauw tall tower site. Atmos. Chem. Phys. 16, 10469–10487. https://doi.org/10.5194/acp-16-10469-2016.

Sherwood, O.A., Schwietzke, S., Arling, V.A., Etiope, G., 2017. Global inventory of gas geochemistry data from fossil fuel, microbial and burning sources. version 2017. Earth System Science Data. https://doi.org/10.5194/essd-9-639-2017.

Swarthout, R.F., Russo, R.S., Zhou, Y., Miller, B.M., Mitchell, B., Horsman, E., Lipsky, E., McCabe, D.C., Baum, E., Sive, B.C., 2020. Impact of Marcellus shale natural gas development in southwest Pennsylvania on volatile organic compound emissions and regional air quality. Environ. Sci. Technol. 49 (5), 3175–3184. https://doi.org/10.1021/es504315f.

Townsend-Small, A., Claire Botner, E., Jimenez, K.L., Schroeder, J.R., Blake, N.J., Meinardi, S., Blake, D.R., Sive, B.C., Bon, D., Crawford, J.H., Pfister, G., Flocke, F.M., 2016a. Using stable isotopes of hydrogen to quantify biogenic and thermogenic atmospheric methane sources: a case study from the Colorado Front Range. Geophys. Res. Lett. https://doi.org/10.1002/2016gl071438.

Townsend-Small, A., Marrero, J.E., Lyon, D.R., Simpson, I.J., Meinardi, S., Blake, D.R., 2015. Integrating source apportionment tracers into a bottom-up inventory of methane emissions in the barnett shale hydraulic fracturing region. Environ. Sci. Technol. https://doi.org/10.1021/acs.est.5b00057.

Townsend-Small, A., Botner, E.C., Jimenez, K.L., Schroeder, J.R., Blake, N.J., Meinardi, S., Blake, D.R., Sive, B.C., Bon, D., Crawford, J.H., Pfister, G., Flocke, F.M., 2016b. Using stable isotopes of hydrogen to quantify biogenic and thermogenic atmospheric methane sources: a case study from the Colorado Front Range. Geophys. Res. Lett. 43 (11), 462–471. https://doi.org/10.1002/2016GL071438.

Tyler, S.C., Rice, A.L., Ajie, H.O., 2007. Stable isotope ratios in atmospheric CH4: implications for seasonal sources and sinks. J. Geophys. Res. Atmos. https://doi.org/10.1029/2006JD007231.

Vardag, S.N., Hammer, S., Levin, I., 2016. Evaluation of 4 years of continuous δ13C(CO2) data using a moving Keeling plot method. Biogeosciences. https://doi.org/10.5194/bg-13-4237-2016.

Vaughn, T.L., Bell, C.S., Pickering, C.K., Schwietzke, S., Heath, G.A., Pétron, G., Zimmerle, D.J., Schnell, R.C., Nummedal, D., 2018. Temporal variability largely explains top-down/bottom-up difference in methane emission estimates from a natural gas production region. In: Proceedings of the National Academy of Sciences. https://doi.org/10.1073/pnas.1805687115.

Vesala, T., Kljun, N., Rannik, Ü., Rinne, J., Sogachev, A., Markkanen, T., Sabelfeld, K., Foken, T., Leclear, M.Y., 2008. Flux and concentration footprint modelling: state of the art. Environ. Pollut. https://doi.org/10.1016/j.envpol.2007.06.070.

Villa J, Ju Y, Stephen T, Rey-Sanchez AC, Bohrer G. (*under review*) Plant-mediated methane transport in emergent and floating-leaved species of a temperate freshwater mineral-soil wetland. J. Geophys. Res. Biogeosci.

White, J.W.C., Vaughn, B.H., Michel, S.E., 2018. University of Colorado, Institute of Arctic and Alpine Research (INSTAAR), Stable Isotopic Composition of Atmospheric Methane (13C) from the NOAA ESRL Carbon Cycle Cooperative Global Air Sampling Network, pp. 1998–2017.

Williams, P.J., Reeder, M., Pekney, N.J., Risk, D., Osborne, J., McCawley, M., 2018. Atmospheric impacts of a natural gas development within the urban context of Morgantown, West Virginia. Sci. Total Environ. 639, 406–416. https://doi.org/10.1016/j.scitotenv.2018.04.422.

Yacovitch, T.I., Daube, C., Herndon, S.C., 2020. Methane emissions from offshore oil and gas platforms in the Gulf of Mexico. Environ. Sci. Technol. 54, 3530–3538. https://doi.org/10.1021/acs.est.9b07148.